ANNALS OF FACULTY ENGINEERING HUNEDOARA
- INTERNATIONAL JOURNAL OF ENGINEERING
Tome IX (Year 2011). Fascicule 3. (ISSN 1584 - 2673)

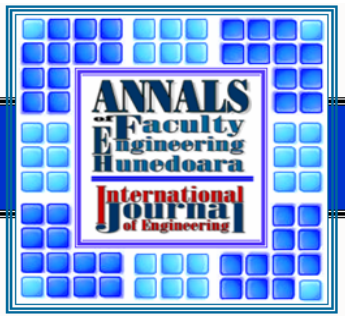

[1.] R. MUTHUCUMARASWAMY, [2.] KE. SATHAPPAN

FINITE DIFFERENCE SOLUTION OF HEAT AND MASS TRANSFER EFFECTS ON FLOW PAST AN OSCILLATING SEMI-INFINITE VERTICAL PLATE WITH THERMAL RADIATION

[1.] DEPARTMENT OF APPLIED MATHEMATICS, SRI VENKATESWARA COLLEGE OF ENGINEERING, PENNALUR, SRIPERUMBUDUR, INDIA.
[2.] DEPARTMENT MATHEMATICS, THIRU. VI. KA. GOVT. ARTS COLLEGE, TIRUVARUR, INDIA

ABSTRACT: Heat and mass transfer effects of thermal radiation on unsteady flow past an oscillating semi-infinite isothermal vertical plate in the presence of thermal radiation have been studied. The fluid considered is a gray, absorbing-emitting radiation but non-scattering medium. The dimensionless governing equations are solved by an efficient, more accurate, and unconditionally stable and fast converging implicit scheme. The effect of velocity and temperature for different parameters like thermal radiation, Schmidt number, thermal Grashof number and mass Grashof number are studied. It is observed that the velocity decreases in the presence of thermal radiation.

KEYWORDS: Radiation, isothermal, vertical plate, finite-difference

❖ INTRODUCTION

The study of radiative heat and mass transfer in convective flows is important from many industrial and technological points of view. Mass transfer is one of the most commonly encountered phenomena in chemical industry as well as in physical and biological sciences. When mass transfer takes place in a fluid at rest the mass is transferred purely by molecular diffusion resulting from concentration gradients. For low concentration of the mass in the fluid and low mass transfer rates, the convective heat and mass transfer processes are similar in nature. A number of investigations have already been carried out with combined heat and mass transfer under the assumption of different physical situations. Radiation in free convection has also been studied by many authors because of its applications in many engineering and industrial processes. Examples include nuclear power plant, solar power technology, steel industry, fossil fuel combustion, space sciences applications, etc.

England and Emery [2] have studied the thermal radiation effects of a optically thin gray gas bounded by a stationary vertical plate. Soundalgekar and Takhar [10] have considered the radiative free convective flow of an optically thin gray-gas past a semi-infinite vertical plate. Radiation effect on mixed convection along a isothermal vertical plate were studied by Hossain and Takhar [3]. In all above studies, the stationary vertical plate is considered. Raptis and Perdikis [5] have studied the effects of thermal radiation and free convection flow past a moving infinite vertical plate. Again, Raptis and Perdikis [6] studied thermal radiation effects on moving infinite vertical plate in the presence of mass diffusion. Radiation effects on moving infinite vertical plate with variable temperature were studied by Muthucumaraswamy and Ganesan [4]. The dimensionless governing equations were solved by the Laplace transform technique.

The flow of a viscous, incompressible fluid past an infinite isothermal vertical plate, oscillating in its own plane, was solved by Soundalgekar [7]. The effect on the flow past a vertical oscillating plate due to a combination of concentration and temperature differences was studied extensively by Soundalgekar and Akolkar [8]. The effect of mass transfer on the flow past an infinite vertical oscillating plate in the presence of constant heat flux has been studied by Soundalgekar et al. [9].

Analytical or numerical work on transient natural convection along an oscillating isothermal vertical plate under the combined buoyancy effects of heat and mass diffusion in the presence of thermal radiation has not received attention of any researcher. Hence, the present study is to investigate the unsteady flow past an oscillating semi-infinite vertical plate with thermal radiation by an implicit finite-difference scheme of Crank-Nicolson type.

❖ MATHEMATICAL FORMULATION

A transient, laminar, unsteady natural convection flow of a viscous incompressible fluid past an oscillating semi-infinite isothermal vertical plate in the presence of thermal radiation has been considered. It is assumed that the concentration C' of the diffusing species in the binary mixture is very in comparison to the other chemical species which are present. Here, the x-axis is taken along the plate in the vertically upward direction and the y-axis is taken normal to the plate. Initially, it is assumed that the plate and the fluid are of the same temperature and concentration. At time $t' > 0$, the plate starts oscillating in its own plane with frequency ω' against gravitational field and the temperature of the plate and the concentration level near the plate are also raised to T_w and C_w'. The fluid considered here is a gray, absorbing-emitting radiation but a non-scattering medium and the viscous dissipation is assumed to be negligible. Then under the above assumptions, the governing boundary layer equations of mass, momentum and concentration for free convective flow with usual Boussinesq's approximation are as follows:

$$\frac{\partial u}{\partial x} + \frac{\partial v}{\partial y} = 0 \tag{1}$$

$$\frac{\partial u}{\partial t'} + u\frac{\partial u}{\partial x} + v\frac{\partial u}{\partial y} = g\beta(T - T_\infty) + g\beta^*(C' - C'_\infty) + \nu\frac{\partial^2 u}{\partial y^2} \tag{2}$$

$$\rho C_p\left(\frac{\partial T}{\partial t'} + u\frac{\partial T}{\partial x} + v\frac{\partial T}{\partial y}\right) = \frac{\partial^2 T}{\partial y^2} - \frac{\partial q_r}{\partial y} \tag{3}$$

$$\frac{\partial C'}{\partial t'} + u\frac{\partial C'}{\partial x} + v\frac{\partial C'}{\partial y} = D\frac{\partial^2 C'}{\partial y^2} \tag{4}$$

The initial and boundary conditions are

$$\begin{array}{llllll} t' \le 0: & u = 0, & v = 0, & T = T_\infty, & C' = C'_\infty & \\ t' > 0: & u = u_0 Cos\omega' t', & v = 0, & T = T_w, & C' = C'_w & at \quad y = 0 \\ & u = 0, & & T = T_\infty, & C' = C'_\infty & at \quad x = 0 \\ & u \to 0, & & T \to T_\infty, & C' \to C'_\infty & as \quad y \to \infty \end{array} \tag{5}$$

For the case of an optically thin gray gas the local radiant absorption is expressed by

$$\frac{\partial q_r}{\partial y} = -4a^*\sigma\left(T_\infty^4 - T^4\right) \tag{6}$$

We assume that the temperature differences within the flow are sufficiently small such that T^4 may be expressed as a linear function of the temperature. This is accomplished by expanding T^4 in a Taylor series about T_∞ and neglecting higher-order terms, thus

$$T^4 \cong 4T_\infty^3 T - 3T_\infty^4 \tag{7}$$

By using equations (6) and (7), equation (3) reduces to

$$\rho C_p\frac{\partial T}{\partial t'} = k\frac{\partial^2 T}{\partial y^2} + 16a^*\sigma T_\infty^3(T_\infty - T) \tag{8}$$

On introducing the following non-dimensional quantities

$$\begin{gathered} U = \frac{u}{u_0}, V = \frac{v}{u_0}, t = \frac{t'u_0^2}{\nu}, X = \frac{xu_0}{\nu} Y = \frac{yu_0}{\nu}, \theta = \frac{T - T_\infty}{T_w - T_\infty}, \\ Gr = \frac{g\beta\nu(T_w - T_\infty)}{u_0^3}, C = \frac{C' - C'_\infty}{C'_w - C'_\infty}, Gc = \frac{\nu g\beta^*(C'_w - C'_\infty)}{u_0^3}, \omega = \frac{\omega'\nu}{u_0^2}, \\ R = \frac{16a^*\nu^2\sigma T_\infty^3}{ku_0^2}, Pr = \frac{\mu C_p}{k}, Sc = \frac{\nu}{D} \end{gathered} \tag{9}$$

Equations (1) to (4) are reduced to the following non-dimensional form

$$\frac{\partial U}{\partial X} + \frac{\partial V}{\partial Y} = 0 \tag{10}$$

$$\frac{\partial U}{\partial t} + U\frac{\partial U}{\partial X} + V\frac{\partial U}{\partial Y} = Gr\,\theta + Gc\,C + \frac{\partial^2 U}{\partial Y^2} \tag{11}$$

$$\frac{\partial T}{\partial t} + U\frac{\partial T}{\partial X} + V\frac{\partial T}{\partial Y} = \frac{1}{\Pr}\frac{\partial^2 T}{\partial Y^2} - \frac{R}{\Pr}T \qquad (12)$$

$$\frac{\partial C}{\partial t} + U\frac{\partial C}{\partial X} + V\frac{\partial C}{\partial Y} = \frac{1}{Sc}\frac{\partial^2 C}{\partial Y^2} \qquad (13)$$

The corresponding initial and boundary conditions in non-dimensional quantities are

$t \le 0$: U = 0, V = 0, T = 0, C = 0

$t > 0$: U = Cosωt, V = 0, T = 1, C =1 at Y = 0 (14)

U = 0, T = 0, C = 0 at X = 0

$U \to 0$, $T \to 0$, $C \to 0$ as $Y \to \infty$

❖ NUMERICAL TECHNIQUE

In order to solve the unsteady, non-linear coupled equations (10) to (13) under the conditions (14), an implicit finite difference scheme of Crank- Nicolson type has been employed. The finite difference equations corresponding to equations (10) to (13) are as follows.

$$\frac{\left[U_{i,j}^{n+1} - U_{i-1,j}^{n+1} + U_{i,j}^{n} - U_{i-1,j}^{n} + U_{i,j-1}^{n+1} - U_{i-1,j-1}^{n+1} + U_{i,j-1}^{n} - U_{i-1,j-1}^{n}\right]}{4\Delta X} + \frac{\left[V_{i,j}^{n+1} - V_{i,j-1}^{n+1} + V_{i,j}^{n} - V_{i,j-1}^{n}\right]}{2\Delta Y} = 0 \qquad (15)$$

$$\frac{\left[U_{i,j}^{n+1} - U_{i,j}^{n}\right]}{\Delta t} + U_{i,j}^{n}\frac{\left[U_{i,j}^{n+1} - U_{i-1,j}^{n+1} + U_{i,j}^{n} - U_{i-1,j}^{n}\right]}{2\Delta X} + V_{i,j}^{n}\frac{\left[U_{i,j+1}^{n+1} - U_{i,j-1}^{n+1} + U_{i,j+1}^{n} - U_{i,j-1}^{n}\right]}{4\Delta Y} \qquad (16)$$

$$= \frac{Gr}{2}\left[T_{i,j}^{n+1} + T_{i,j}^{n}\right] + \frac{Gc}{2}\left[C_{i,j}^{n+1} + C_{i,j}^{n}\right] + \frac{\left[U_{i,j-1}^{n+1} - 2U_{i,j}^{n+1} + U_{i,j+1}^{n+1} + U_{i,j-1}^{n} - 2U_{i,j}^{n} + U_{i,j+1}^{n}\right]}{2(\Delta Y)^2}$$

$$\frac{\left[T_{i,j}^{n+1} - T_{i,j}^{n}\right]}{\Delta t} + U_{i,j}^{n}\frac{\left[T_{i,j}^{n+1} - T_{i-1,j}^{n+1} + T_{i,j}^{n} - T_{i-1,j}^{n}\right]}{2\Delta X} + V_{i,j}^{n}\frac{\left[T_{i,j+1}^{n+1} - T_{i,j-1}^{n+1} + T_{i,j+1}^{n} - T_{i,j-1}^{n}\right]}{4\Delta Y}$$

$$= \frac{1}{Pr}\frac{\left[T_{i,j-1}^{n+1} - 2T_{i,j}^{n+1} + T_{i,j+1}^{n+1} + T_{i,j-1}^{n} - 2T_{i,j}^{n} + T_{i,j+1}^{n}\right]}{2(\Delta Y)^2} - \frac{R(T_{i,j}^{n+1} + T_{i,j}^{n})}{2Pr} \qquad (17)$$

$$\frac{\left[C_{i,j}^{n+1} - C_{i,j}^{n}\right]}{\Delta t} + U_{i,j}^{n}\frac{\left[C_{i,j}^{n+1} - C_{i-1,j}^{n+1} + C_{i,j}^{n} - C_{i-1,j}^{n}\right]}{2\Delta X} + V_{i,j}^{n}\frac{\left[C_{i,j+1}^{n+1} - C_{i,j-1}^{n+1} + C_{i,j+1}^{n} - C_{i,j-1}^{n}\right]}{4\Delta Y}$$

$$= \frac{1}{Sc}\frac{\left[C_{i,j-1}^{n+1} - 2C_{i,j}^{n+1} + C_{i,j+1}^{n+1} + C_{i,j-1}^{n} - 2C_{i,j}^{n} + C_{i,j+1}^{n}\right]}{2(\Delta Y)^2} \qquad (18)$$

Here the region of integration is considered as a rectangle with sides X_{max} (= 1) and Y_{max} (=14), where Y_{max} corresponds to Y = ∞ which lies very well outside both the momentum and energy boundary layers. The maximum of Y was chosen as 14 after some preliminary investigations so that the last two of the boundary conditions (14) are satisfied with in the tolerance limit 10^{-5}.

After experimenting with a few set of mesh sizes have been fixed at the level $\Delta X = 0.05$, $\Delta Y = 0.25$, with time step $\Delta t = 0.01$. In this case, the spatial mesh sizes are reduced by 50% in one direction, and later in both directions, and the results are compared. It is observed that, when the mesh size is reduced by 50% in the Y-direction, the results differ in the fifth decimal place while the mesh sizes are reduced by 50% in X-direction or in both directions, the results are comparable to three decimal places. Hence, the above mesh sizes have been considered as appropriate for calculation. The coefficients $U_{i,j}^{n}$ and $V_{i,j}^{n}$ appearing in the finite difference equation are treated as constants at any one time step. Here i-designates the grid point along the X - direction, j along the Y- direction and k to the t-time.The values of U, V and T are known at all grid points at t = 0 from the initial conditions.

The computations of U, V , T and C at time level (n +1) using the values at previous time level (n) are carried out as follows: The finite-difference equation (18) at every internal nodal point on a particular i-level constitute a tridiagonal system of equations. Such a system of equations is solved by using Thomas algorithm as discusses in Carnahan et al [1]. Thus, the values of C are found at every nodal point for a particular i at $(n+1)^{th}$ time level. Similarly, the values of T are calculated from equation (17) .Using the values of C and T at $(n+1)^{th}$ time level in the equation (16) , the values of U at $(n+1)^{th}$ time level are found in a similar manner. Thus, the values of C, T and U are known on a particular i-level. Finally, the values of V are calculated explicitly using the equation (15) at every nodal point at particular i-level at $(n+1)^{th}$ time level. This process is repeated for various i-levels. Thus the values of C, T, U and V are known, at all grid points in the rectangle region at $(n+1)^{th}$ time level.

In a similar manner computations are carried out by moving along the i-direction. After computing values corresponding to each i at a time level, the values at the next time level are determined in a similar manner. Computations are repeated until the steady-state is reached. The

steady-state solution is assumed to have been reached, when the absolute difference between the values of U, and as well as temperature T and concentration C at two consecutive time steps are less than 10^{-5} at all grid points.

❖ STABILITY ANALYSIS

The stability criterion of the finite difference scheme for constant mesh sizes are examined using Von-Neumann technique as explained by Carnahan et al.[1]. The general term of the Fourier expansion for U, T and C at a time arbitrarily called t = 0, are assumed to be of the form exp (i α X) exp (i β Y) (here i = $\sqrt{-1}$). At a later time t, these terms will become,

$$\begin{aligned} U &= F(t)\exp(i\alpha X)\exp(i\beta Y) \\ T &= G(t)\exp(i\alpha X)\exp(i\beta Y) \\ C &= H(t)\exp(i\alpha X)\exp(i\beta Y) \end{aligned} \tag{19}$$

Substituting (19) in Equations (16) to (18); under the assumption that the coefficients U, T and C are constants over any one time step and denoting the values after one time step by F', G' and H'. After simplification, we get

$$\frac{(F'-F)}{\Delta t}+\frac{U}{2}\frac{(F'+F)(1-\exp(-i\alpha\Delta X))}{\Delta X}+\frac{V}{2}\frac{(F'+F)i\sin\beta\Delta Y}{\Delta Y} = \frac{(G'+G)Gr+(H'+H)Gc-M(F'+F)}{2}+\frac{(F'+F)(\cos\beta\Delta Y-1)}{(\Delta Y)^2} \tag{20}$$

$$\frac{(G'-G)}{\Delta t}+\frac{U}{2}\frac{(G'+G)(1-\exp(-i\alpha\Delta X))}{\Delta X}+\frac{V}{2}\frac{(G'+G)i\sin\beta\Delta Y}{\Delta Y} = \frac{1}{\Pr}\frac{(G'+G)(\cos\beta\Delta Y-1)}{(\Delta Y)^2}-\frac{R}{2\Pr}(G'+G) \tag{21}$$

$$\frac{(H'-H)}{\Delta t}+\frac{U}{2}\frac{(H'+H)(1-\exp(-i\alpha\Delta X))}{\Delta X}+\frac{V}{2}\frac{(H'+H)i\sin\beta\Delta Y}{\Delta Y} = \frac{1}{Sc}\frac{(H'+H)(\cos\beta\Delta Y-1)}{(\Delta Y)^2} \tag{22}$$

Equations (20) to (22) can be rewritten as,

$$(1+A)F' = (1-A)F+\frac{Gr}{2}(G'+G)\Delta t+\frac{Gc}{2}(H'+H)\Delta t \tag{23}$$

$$(1+B)G' = (1-B)G \tag{24}$$

$$(1+E)H' = (1-E)H \tag{25}$$

where,

$$A = \frac{U}{2}\frac{\Delta t}{\Delta X}(1-\exp(-i\alpha\Delta X))+\frac{V}{2}\frac{\Delta t}{\Delta Y}i\sin(\beta\Delta Y)-(\cos\beta\Delta Y-1)\frac{\Delta t}{(\Delta Y)^2}$$

$$B = \frac{U}{2}\frac{\Delta t}{\Delta X}(1-\exp(-i\alpha\Delta X))+\frac{V}{2}\frac{\Delta t}{\Delta Y}i\sin\beta\Delta Y-\frac{(\cos\beta\Delta Y-1)}{\Pr}\frac{\Delta t}{(\Delta Y)^2}+\frac{R\Delta t}{2\Pr}$$

$$E = \frac{U}{2}\frac{\Delta t}{\Delta X}(1-\exp(-i\alpha\Delta X))+\frac{V}{2}\frac{\Delta t}{\Delta Y}i\sin\beta\Delta Y-\frac{(\cos\beta\Delta Y-1)}{Sc}\frac{\Delta t}{(\Delta Y)^2}$$

After eliminating G' and H' in Equation (23) using Equations (24) and (25),the resultant equation is given by,

$$(1+A)F' = (1-A)F+G\frac{Gr\Delta t}{(1+B)}+H\frac{Gc\Delta t}{(1+E)} \tag{26}$$

Equations (23) to (25) can be written in matrix form as follows:

$$\begin{bmatrix} F' \\ G' \\ H' \end{bmatrix} = \begin{bmatrix} \frac{1-A}{1+A} & D_1 & D_2 \\ 0 & \frac{1-B}{1+B} & 0 \\ 0 & 0 & \frac{1-E}{1+E} \end{bmatrix} \begin{bmatrix} F \\ G \\ H \end{bmatrix} \tag{27}$$

where, $D_1 = \dfrac{Gr\,\Delta t}{(1+A)(1+B)}$ and $D_2 = \dfrac{Gc\,\Delta t}{(1+A)(1+E)}$

Now, for stability of the finite difference scheme, the modulus of each eigen value of the amplification matrix does not exceed unity. Since the matrix Equation (27) is triangular, the eigen values are its diagonal elements. The eigen values of the amplification matrix are $(1-A)/(1+A)$, $(1-B)/(1+B)$ and $(1-E)/(1+E)$. Assuming that, U is everywhere non-negative and V is everywhere non-positive, we get

$$A = 2a\sin^2\left(\frac{\alpha\Delta X}{2}\right) + 2c\sin^2\left(\frac{\beta\Delta Y}{2}\right) + i(a\sin\alpha\Delta X - b\sin\beta\Delta Y) + d$$

where, $a = \frac{U}{2}\frac{\Delta t}{\Delta X}$, $b = \frac{|V|}{2}\frac{\Delta t}{\Delta Y}$, $c = \frac{\Delta t}{(\Delta Y)^2}$

Since the real part of A is greater than or equal to zero, $\left|(1-A)/(1+A)\right| \le 1$ always. Similarly, $\left|(1-B)/(1+B)\right| \le 1$ and $\left|(1-E)/(1+E)\right| \le 1$.

Hence the finite difference scheme is unconditionally stable. The local truncation error is $O(\Delta t^2 + \Delta Y^2 + \Delta X)$ and it tends to zero as Δt , ΔX and ΔY tend to zero. Hence the scheme is compatible. Stability and compatibility ensures convergence.

❖ RESULTS AND DISCUSSION

The numerical values of the velocity, temperature and concentation are computed for different parameters like radiation parameter, Schmidt number, thermal Grashof number and mass Grashof number. The purpose of the calculations given here is to assess the effects of the parameters R, Gr, Gc and Sc upon the nature of the flow and transport. The value of Prandtl number Pr is chosen such that they represent air (Pr = 0.71) and the Schmidt number Sc = 0.6(Water vapour).

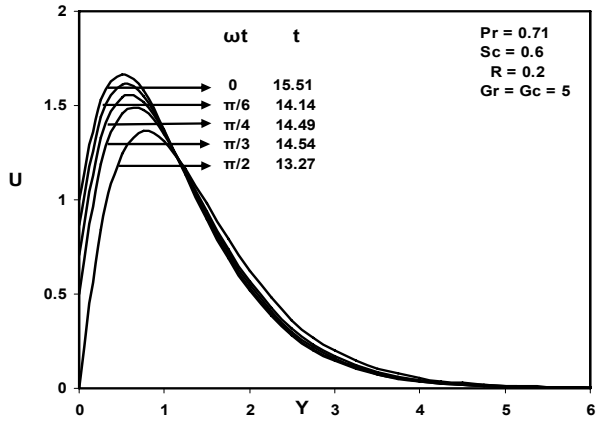

Figure 1. Steady state velocity profiles for different values of ωt

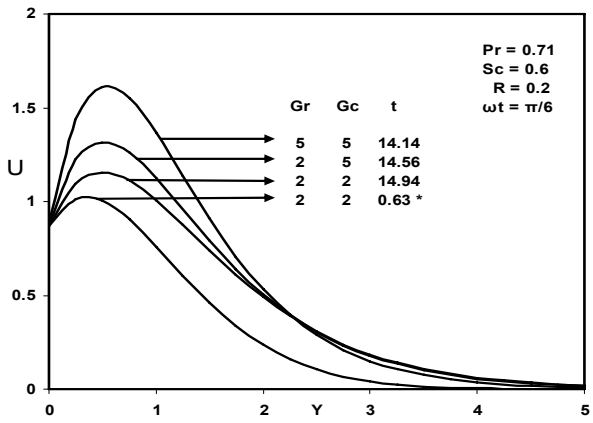

Figure 2. Steady state velocity profiles for different values of Gr & Gc (* transient state)

The steady-state velocity profiles for different phase angle are shown in figure 1. The velocity profiles presented are those at X = 1.0. It is observed that for different phase angle ($\omega t = 0, \pi/6, \pi/4, \pi/3, \pi/2$), the velocity decreases with increasing phase angle. Here ωt = 0 represents vertical plate and note that the velocity profile grows from U = 1 and $\omega t = \pi/2$ refers horizontal plate and the velocity profiles starting with U = 0. The numerical value satisfies with the prescribed boundary conditions. The time to reach steady-state strongly depends on phase angle.

In figure 2, the velocity profiles for different thermal Grashof number and mass Grashof number are shown graphically. This shows that the velocity increases with increasing thermal Grashof number or mass Grashof number. As thermal Grashof number or mass Grashof number increases, the buoyancy effect becomes more significant, as expected; it implies that, more fluid is entrained from the free stream due to the strong buoyancy effects.

The effect of velocity for different radiation parameter (R = 2, 5, 10), and Sc = 0.6 are shown in figure 3. It is observed that the velocity increases with decreasing radiation parameter. This shows that velocity decreases in the presence of high thermal radiation.

The transient and steady-state velocity profiles for different Schmidt number are shown in figure 4. The velocity profiles presented are those at X = 1.0. It is observed that the velocity decreases with increasing Schmidt number and the steady-state value increases with increasing Schmidt number. The velocity boundary layer seems to grow in the direction of motion of the plate. It is observed that near the leading edge of a semi-infinite vertical plate moving in a fluid, the boundary layer develops along the direction of the plate. However, the time required for the velocity to reach steady-state depends

upon the Schmidt number. This shows that the contribution of mass diffusion to the buoyancy force increases the maximum velocity significantly.

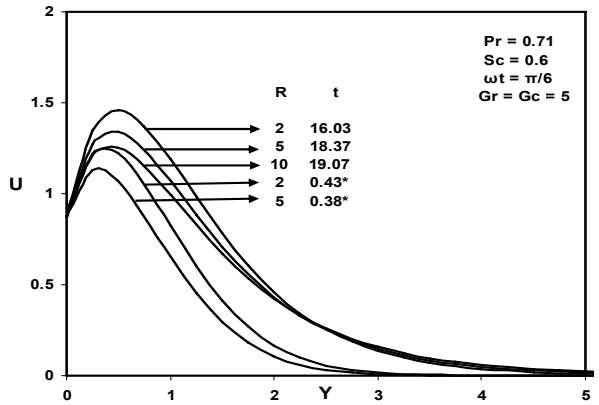

Figure 3. Steady state velocity profiles for different values of R (* transient state)

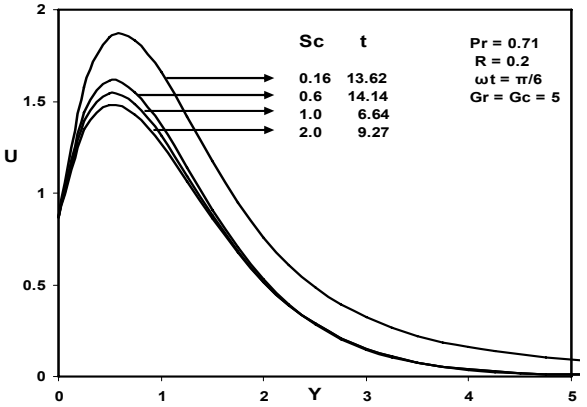

Figure 4. Steady state velocity profiles for different values of Sc

The transient temperature profiles for different values of the thermal radiation parameter are shown in figure 5. It is observed that the temperature increases with decreasing R. This shows that the buoyancy effect on the temperature distribution is very significant in air (Pr = 0.71). It is known that the radiation parameter and Prandtl number plays an important role in flow phenomena because, it is a measure of the relative magnitude of viscous boundary layer thickness to the thermal boundary layer thickness.

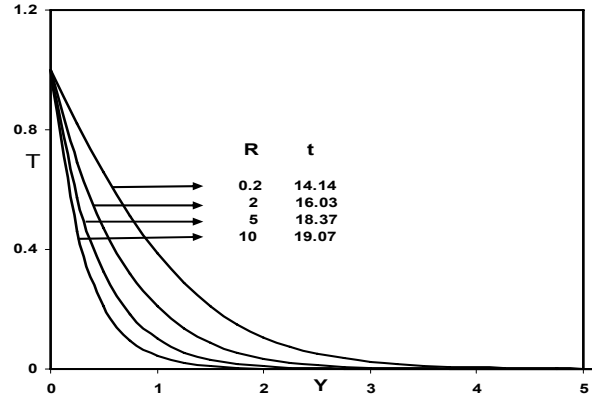

Figure 5. Temperature profiles for different values of R

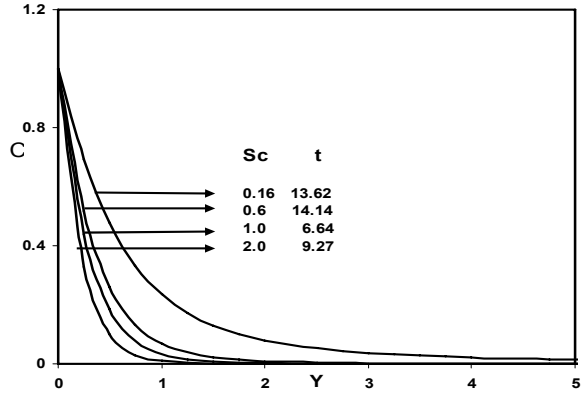

Figure 6. Concentration profiles for different values of Sc

Knowing the velocity and temperature field, it is customary to study the skin-friction and the Nusselt number. The local as well as average values of skin-friction and Nusselt number in dimensionless form are as follows:

$$\tau_X = -\left(\frac{\partial U}{\partial Y}\right)_{Y=0} \tag{28}$$

$$\bar{\tau} = -\int_0^1 \left(\frac{\partial U}{\partial Y}\right)_{Y=0} dX \tag{29}$$

$$Nu_X = \frac{-X\left(\frac{\partial T}{\partial Y}\right)_{Y=0}}{T_{Y=0}} \tag{30}$$

$$\overline{Nu} = -\int_0^1 \left[\frac{\left(\frac{\partial T}{\partial Y}\right)_{Y=0}}{T_{Y=0}}\right] dX \tag{31}$$

$$Sh_X = -X\left(\frac{\partial C}{\partial Y}\right)_{Y=0} \tag{32}$$

$$\overline{Sh} = -\int_0^1 \left(\frac{\partial C}{\partial Y}\right)_{Y=0} dX \tag{33}$$

The derivatives involved in the Equations (28) to (33) are evaluated using five-point approximation formula and then the integrals are evaluated using Newton-Cotes closed integration formula.

The local skin-friction, Nusselt number and Sherwood number are plotted in figures 6, 7 and 8 respectively. Local skin-friction values for different phase angle are evaluated from equation (28) and plotted in figure 7 as a function of the axial coordinate. The local wall shear stress increases with decreasing phase angle. The trend shows that the wall shear stress is more in the case of vertical plate than horizontal plate. The value of the skin-friction becomes negative, which implies, that after some time there occurs a reverse type of flow near the oscillating plate. Physically this is also true as the motion of the fluid is due to plate moving in the vertical direction against the gravitational field.

The local Nusselt number for different thermal radiation parameter is presented in figure 8 as a function of the axial co-ordinate. The trend shows that the Nusselt number increase with increasing values of the thermal radiation parameter. It is clear that the rate of heat transfer is more in the presence of thermal radiation.

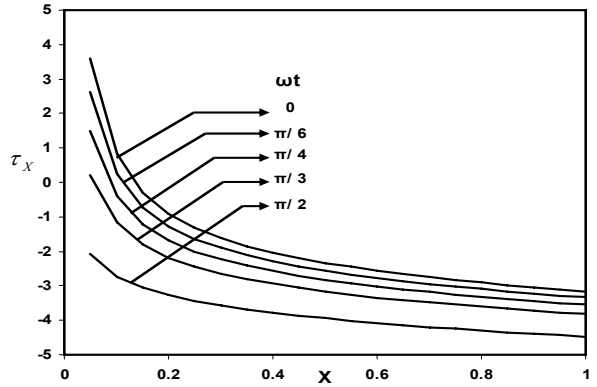

Figure 7. Local Skin-friction

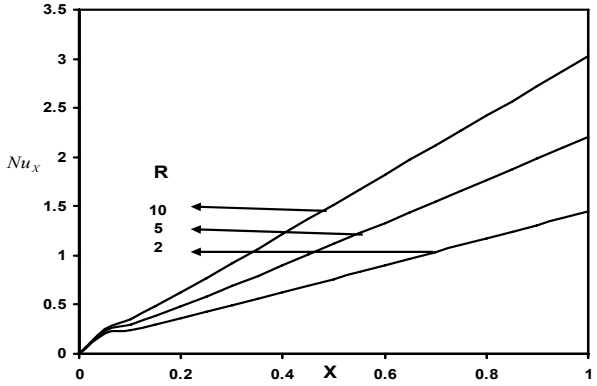

Figure 8. Local Nusselt number

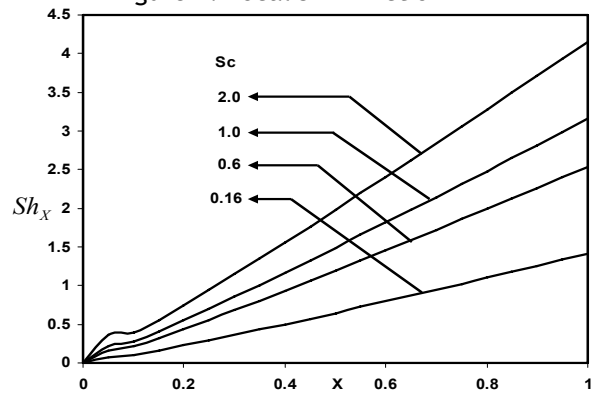

Figure 9. Local Sherwood number

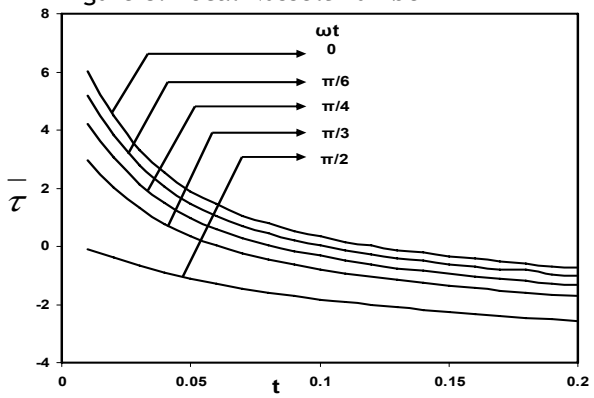

Figure 10. Average Skin – friction

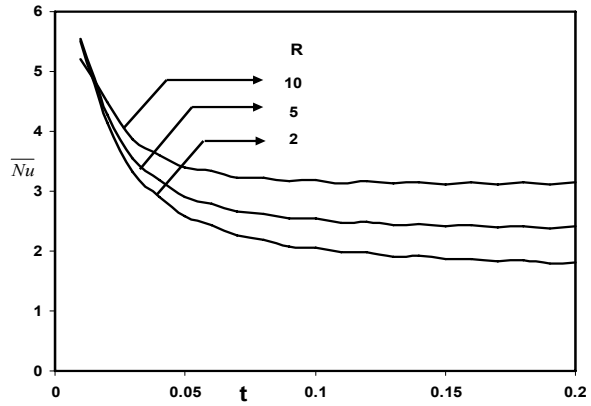

Figure 11. Average Nusselt number

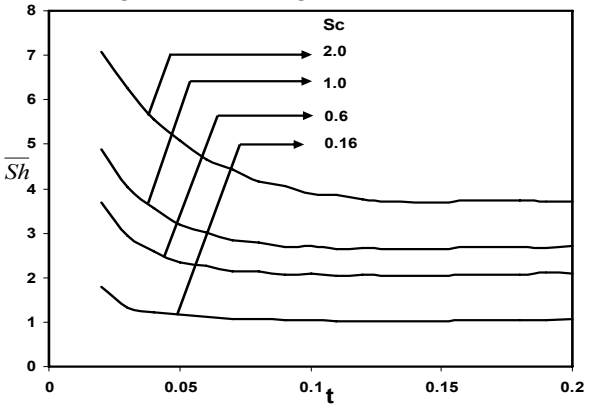

Figure 12. Average Sherwood number

The local Sherwood number for different values of the Schmidt number are shown in figure 9. As expected, the rate of mass transfer increases with increasing values of the Schmidt number. This trend is just reversed as compared to the concentration field for different Schmidt number given in figure 6.

The average values of the skin-friction, Nusselt number and Sherwood number are shown in figures 10, 11 and 12 respectively. The effects of the different phase angle on the average values of the skin-friction are shown in figure 10. The average skin-friction decreases with decreasing with increasing values of the phase angle. Figure 11 illustrates the average Nusselt number increases with increasing radiation parameter. From figure 12, It is observed that the average Sherwood number increases with increasing values of the Schmidt number.

❖ CONCLUSIONS

Finite difference study has been carried out for unsteady flow past an oscillating semi-infinite isothermal vertical plate in the presence of thermal radiation. The dimensionless governing equations are solved by an implicit scheme of Crank-Nicolson type. The effect of velocity, temperature and concentration for different parameter are studied. The local as well as average skin-friction, Nusselt number and Sherwood number are shown graphically. It is observed that the contribution of mass diffusion to the buoyancy force increases the maximum velocity significantly. It is also observed that the velocity decreases in the presence of thermal radiation. The study shows that the number of time steps to reach steady-state depends strongly on the radiation parameter.

❖ ACKNOWLEDGEMENT

The first author thanks Defence Research Development Organisation (DRDO), Government of India, for its financial support through extramural research grant.

❖ REFERENCES

[1.] CARNAHAN B., LUTHER H.A. and WILKES J.O., Applied Numerical Methods, John Wiley and sons, New York, 1969.
[2.] ENGLAND W.G. and EMERY A.F., Thermal radiation effects on the laminar free convection boundary layer of an absorbing gas, J. Heat transfer, Vol. 91, pp. 37-44, 1969.
[3.] HOSSIAN M.A. and TAKHAR H.S., Radiation effect on mixed convection along a vertical plate with uniform surface temperature, Heat and mass Transfer, Vol.31, pp.243-248, 1996.
[4.] MUTHUCUMARASWAMY R. and GANESAN P., Radiation effects on flow past an impulsively started infinite vertical plate with variable temperature, International Journal of Applied Mechanics and Engineering Vol.8, 125-129, 2003.
[5.] RAPTIS A. and PERDIKIS C., Radiation and free convection flow past a moving plate, Int. J. App. Mech. and Engg., Vol. 4, pp.817-821, 1999.
[6.] RAPTIS A. and PERDIKIS C., Thermal radiation of an optically thin gray gas, Int. J. App. Mech. and Engg., Vol. 8, pp.131-134, 2003.
[7.] SOUNDALGEKAR V. M., Free convection effects on the flow past a vertical oscillating plate, Astrophysics and Space Science, Vol.64, pp.165-172, 1979.
[8.] SOUNDALGEKAR V. M and AKOLKAR S.P., Effects of free convection currents and mass transfer on the flow past a vertical oscillating plate, Astrophysics and Space Science, Vol.89, pp.241- 254, 1983.
[9.] SOUNDALGEKAR V.M., LAHURIKAR R.M., POHANERKAR S.G. and BIRAJDAR, N.S., Effects of mass transfer on the flow past an oscillating infinite vertical plate with constant heat flux, Thermophysics and AeroMechanics, Vol.1, pp.119-124, 1994.
[10.] SOUNDALGEKAR V.M and TAKHAR H. S., Radiation effects on free convection flow past a semi-infinite vertical plate, Journal of Modeling, Measurements and Control, Vol.B51, pp. 31-40, 1993.

ANNALS OF FACULTY ENGINEERING HUNEDOARA
– INTERNATIONAL JOURNAL OF ENGINEERING